Mitochondrial Encephalomyopathy: Comparison of Conventional MR Imaging with Diffusion-Weighted and Diffusion Tensor Imaging: Case Report

Charles B. Majoie, Erik M. Akkerman, Christian Blank, Peter G. Barth, Bwee Tien Poll-The, and G.J. den Heeten.

Summary: Conventional MR imaging, MR spectroscopy, diffusion-weighted imaging, and diffusion tensor imaging were performed in a 5-month-old male patient with mitochondrial encephalomyopathy. On conventional T2-weighted MR images, symmetric, confluent high signal intensity was found in the temporoparietal white matter. A large lactate peak and decreased *N*-acetylaspartate were found in this region on proton MR spectroscopic images. Diffusion-weighted imaging showed increased apparent diffusion coefficient, representing vasogenic edema. Diffusion tensor imaging revealed decreased anisotropy, consistent with injury to the oligodendro-axonal unit. A muscle biopsy specimen revealed an isolated complex III enzyme respiratory chain deficiency. Diffusion-weighted and diffusion tensor imaging are valuable techniques for the characterization of hyperintense lesions on T2-weighted MR images in cases of mitochondrial encephalomyopathy.

Mitochondrial encephalomyopathies are a heterogeneous group of disorders affecting primarily the CNS and skeletal muscle (1). The diagnosis of the mitochondrial disorder is based on polarographic and spectrophotometric studies and histopathologic analysis of muscle specimens. Molecular genetic studies may reveal mitochondrial or nuclear DNA mutations (1). On conventional T2-weighted MR images, increased signal intensity in gray and white matter structures can occasionally be found (2, 3). These hyperintense lesions do not usually follow vascular territories, and pathologic studies do not find lesions of the major cerebral blood vessels (4). Follow-up imaging may show resolution and subsequent reappearance of the white matter lesions (5, 6). The cause of the white matter lesions is not well understood and has been attributed to small vessel ischemia and/or demyelination (7). To further characterize these white matter abnormalities, we performed diffusion-weighted and diffusion tensor imaging in a patient with biopsy-proven mitochondrial encephalomyopathy.

Case Report

A 5-month-old male Caucasian patient presented to a general hospital with a 4-day history of vomiting and diarrhea. He was the first child born to nonconsanguineous parents after a term pregnancy and normal delivery. An examination revealed that he was moderately dehydrated. He was treated with IV and orally administered fluid. One week after admission, the infant showed subtle and focal clonic convulsions during a period of 45 min. Serum glucose, electrolytes, and ammonia were normal. CT of the head revealed symmetrical temporoparietal white matter hypoattenuation. The infant was referred to our institution for further investigation.

The patient had poor eye contact, hypotonia with head lag, and otherwise normal growth parameters. Although he experienced no clinical seizures while at our hospital, his EEG results indicated bilateral temporal foci with continuous epileptogenic activity.

MR imaging evaluation of the whole brain was performed on a 1.5-T unit using a standard quadrature head coil. Conventional spin-echo T1-weighted (570/14 [TR/TE]) and fast spin-echo T2-weighted (3500/22, 90 [TR/TE, effective TE]) images were obtained, with an echo train length of 10, a field of view of 23×23 cm, an imaging matrix of 256×256, and a 5-mm section thickness with a 1-mm gap. Diffusion-weighted MR images were acquired with a field of view of 26×26 cm. Section thickness, gap, orientation, and section positions were the same as for the axial T1- and T2-weighted sequences. We used a single-shot, spin-echo, echo-planar imaging sequence, with a TE of 100 and an acquisition matrix of 96×200, reconstructed to 256×256 images. One image with a b value of 0 and six images with a b value of 1000 s/mm2 were acquired, with the diffusion-sensitizing gradient pointing in six non-collinear directions so as to gather complete diffusion tensor data. Between echo-planar image acquisitions, TR was 4000. Based on the acquired data, the average apparent diffusion coefficient (ADC) was calculated (ie, one third of the trace of the diffusion tensor and the fractional anisotropy) (8).

For MR spectroscopy, axial T2-weighted MR images were used to prescribe $2 \times 2 \times 2$ cm voxels. Voxel location was chosen to contain the affected white matter in the left temporal lobe. Data were acquired using a fully automated execution of Proton Brain Examination, developed to acquire and process single voxel proton spectra, as described previously (9). The point-resolved spectroscopy localization technique was used with the following sequence parameters: 3000/35, 144; 128 acquisitions. The spectroscopic data acquisition provides a water-suppressed proton spectrum over a range from 4.3 to 0.5 ppm. The pure metabolic signal was apodized, zero-filled, and Fourier-transformed to produce the spectrum. The numerical analysis was based on peak amplitude by normalizing the line widths of the peaks. This analysis effectively measures areas and ratios of areas. All peaks in the designated spectral area were curve-fitted using a Marquardt fitting routine.

The axial T2-weighted MR images revealed high signal intensity in the swollen temporoparietal white matter of both hemispheres (Fig 1A). MR spectroscopy at a TE of 35 revealed
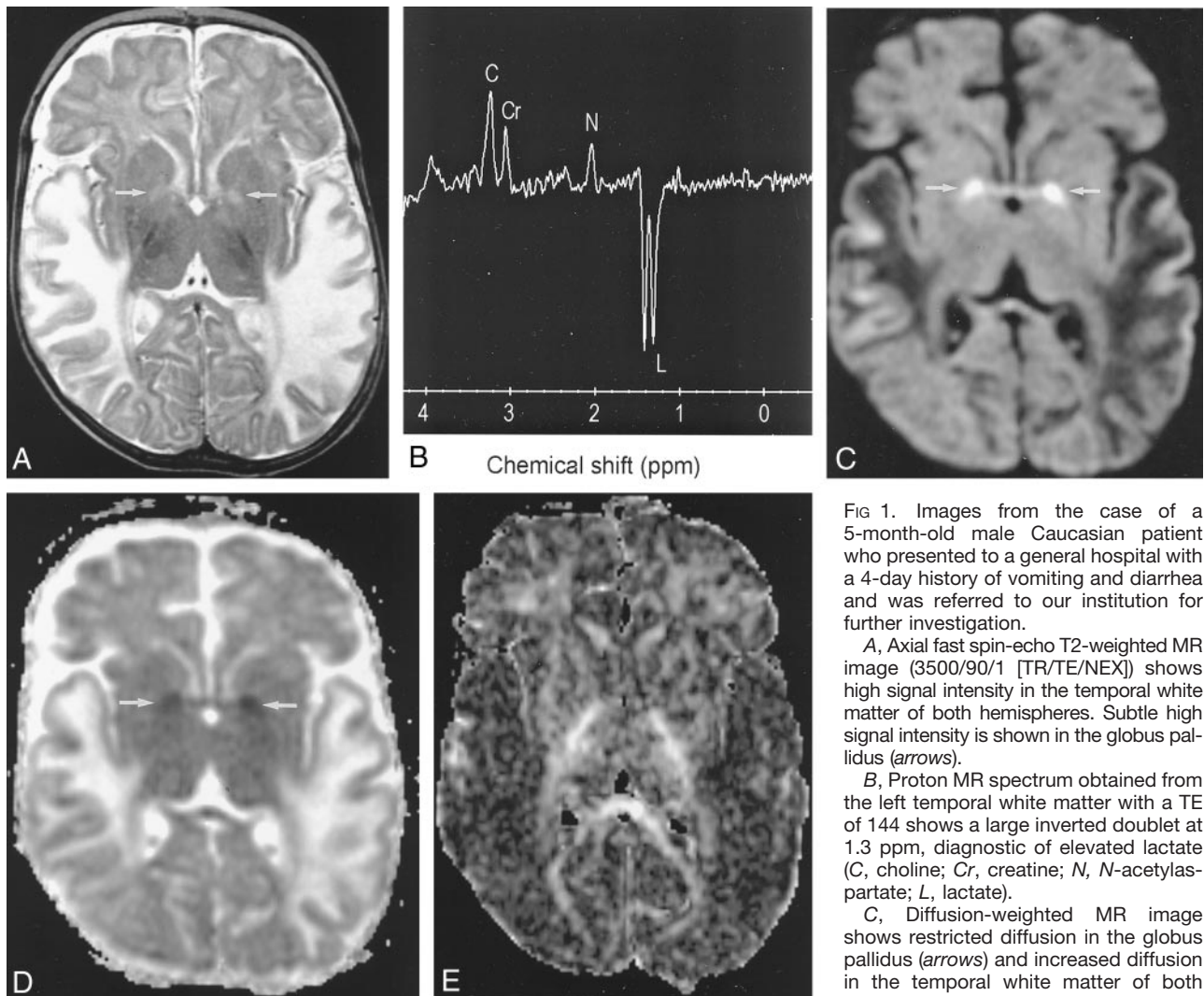
FIG 1. Images from the case of a 5-month-old male Caucasian patient who presented to a general hospital with a 4-day history of vomiting and diarrhea and was referred to our institution for further investigation.

A, Axial fast spin-echo T2-weighted MR image (3500/90/1 [TR/TE/NEX]) shows high signal intensity in the temporal white matter of both hemispheres. Subtle high signal intensity is shown in the globus pallidus (*arrows*).

B, Proton MR spectrum obtained from the left temporal white matter with a TE of 144 shows a large inverted doublet at 1.3 ppm, diagnostic of elevated lactate (*C*, choline; *Cr*, creatine; *N*, *N*-acetylaspartate; *L*, lactate).

C, Diffusion-weighted MR image shows restricted diffusion in the globus pallidus (*arrows*) and increased diffusion in the temporal white matter of both hemispheres.

D, ADC map corresponding to area shown in *C* shows decreased ADC in globus pallidus (*arrows*) and increased ADC in temporal white matter.

E, Fractional anisotropy map shows decreased anisotropy in the temporal white matter.

a large doublet in this region at 1.3 ppm, which was inverted at a TE of 144, diagnostic of lactate. The *N*-acetylaspartate:creatine ratio was reduced (Fig 1B). Diffusion-weighted images showed low signal intensity (increased diffusion) and increased ADC in these areas, consistent with vasogenic edema. In the globi pallidi, high signal intensity was observed on the diffusion-weighted images and low signal intensity on the ADC maps, consistent with cytotoxic edema, as seen in cases of acute infarct (Fig 1C and D). Fractional anisotropy maps of the entire brain revealed decreased anisotropy in the affected temporoparietal areas bilaterally (Fig 1E).

Lactate values in plasma and CSF were increased and gas chromatography mass spectrometry showed elevated urinary lactate, but no metabolic acidosis was present. A muscle biopsy revealed an isolated deficiency of one of the five multienzyme complexes of the respiratory chain, specifically complex III (coenzyme Q-cytochrome C oxidoreductase).

Discussion

In our patient, high signal intensity on T2-weighted MR images was found in the temporoparietal white matter and globus pallidus of both cerebral hemispheres. Two different diffusion abnormalities corresponded with these lesions: restricted diffusion, consistent with cytoxic edema in the globi pallidi, and increased diffusion in the temporoparietal white matter, consistent with vasogenic edema.

The globus pallidus is commonly affected in mitochondrial encephalopathy (10). The relatively high baseline-firing rate of pallidal neurons, which are disinhibited when the rest of the motor system is quiet, could predispose them to selective injury from mitochondrial failure (10).

Areas of increased signal intensity in the white matter on T2-weighted MR images have been described previously in cases of mitochondrial encephalomyopathy (2, 3, 5, 6). The white matter lesions are not necessarily permanent and may resolve. Reappearance may subsequently occur (5, 6). The cause of these white matter hyperintensities is not completely understood. Two main hypotheses have been proposed to explain brain involvement in mitochondrial

encephalomyopathy: angiopathy leading to ischemia and direct neuronal death from mitochondrial impairment (11). The stroke-like abnormalities have been attributed to swelling and increase in number of dysfunctional mitochondria in the smooth muscle and endothelial cells of small arteries and pial arterioles, as revealed by electron microscopy studies (11). Oppenheim et al (4) found increased ADC values in a temporo-occipital lesion in a patient with acute mitochondrial encephalomyopathy, lactic acidosis, and stroke-like episodes. They suggested that there is increased permeability of the blood-brain barrier, presumably based on mitochondrial respiratory failure in the endothelium of small cerebral arteries. Yoneda et al (12) found increased ADC values in a focus with increased T2 signal intensity in the occipital lobe of a patient with acute stage mitochondrial encephalomyopathy, with normal findings of MR angiography (12). ADC values returned to normal 25 days after stroke onset. They suggested that the findings during the acute stage were consistent with vasogenic edema, as opposed to cytotoxic edema. They concluded that the high mobility of protons that was detected by diffusion-weighted imaging supported the idea that there is increased permeability in the blood-brain barrier, presumably based on mitochondrial respiratory failure in the cerebral artery endothelium. Clark et al (13) suggested that impaired metabolic activity of mitochondria in the endothelial and smooth muscle cells of blood vessels may disturb the autoregulatory mechanism, resulting in vasogenic edema, seen as high signal intensity on T2-weighted images. These findings correspond to the findings in the temporoparietal white matter of our patient: low signal intensity on diffusion-weighted images, high signal intensity on ADC maps, consistent with vasogenic edema. Ohshita et al (14) found increased ADC in mitochondrial encephalomyopathy lesions, which disappeared almost completely with clinical improvement. ADC returned to normal levels in these patients.

MR spectroscopy is useful for limiting the large differential diagnosis of diseases causing cerebral white matter abnormalities. The presence of lactate on proton MR spectroscopic images has been reported in association with mitochondrial encephalomyopathies and with cerebral infarction (6). Castillo et al (6) found small lactate peaks in all five patients with mitochondrial encephalomyopathy, lactic acidosis, and stroke-like episodes who underwent MR spectroscopy, despite normal or near normal conventional MR imaging findings. Patients with mitochondrial disorders have deficient oxidative phosphorylation; as a result, anaerobic metabolism uses pyruvate to produce lactate. Elevated lactate may also be due to vascular compromise caused by accumulation of abnormal mitochondria in the endothelium of capillaries and small pial arterioles, the so-called mitochondrial microangiopathy (11).

For our patient, fractional anisotropy maps revealed decreased anisotropy in the temporoparietal white matter. It is possible that fiber destruction and/or demyelination contributed to the decrease in anisotropy in these areas. In the normal brain, diffusion is anisotropic (15). The cause of this anisotropy is not completely understood. It is likely that different factors contribute to anisotropy, including axonal direction, myelination, axolemmelic flow, extracellular bulk flow, capillary blood flow, and intracellular streaming (16). Anisotropic diffusion has been shown to occur before the onset of myelination in the developing rat brain. This premyelination anisotropy seems to be related to some premyelinative changes, including an increase in fiber diameter, axonal membrane changes, and ensheathment of axons by oligodendrocytes (17). Previous authors have suggested that demyelination occurs in mitochondrial encephalomyopathy, probably secondary to degeneration of oligodendrocytes. In an autopsy study of two patients with mitochondrial encephalomyopathy, Ohara et al (18) found microvacuolation of the myelin sheath within the spinal cord. Sandhu and Dillon (7) postulated that as a result of abnormal energy production secondary to mitochondrial dysfunction, the oligodendrocyte may not be able to meet its required energy demands and demyelination may follow. Therefore, the combination of degeneration of oligodendrocytes and demyelination is probably the cause of decreased anisotropy, as shown in our case.

Conclusion

Our case illustrates the added value of diffusion and diffusion tensor imaging for a patient with mitochondrial encephalomyopathy for the characterization of hyperintense abnormalities on T2-weighted MR images. In our case, these areas were consistent with vasogenic edema. In addition, diffusion tensor imaging may reveal injury to the oligodendro-axonal unit, reflected by a decrease in fractional anisotropy in the white matter.

Acknowledgment

References

1. DiMauro S, Moraes CT. **Mitochondrial encephalomyopathies.** *Arch Neurol* 1993;50:1197–1208
2. de Lonlay-Debeney P, von Kleist-Retzow JC, Hertz-Pannier L, et al. **Cerebral white matter disease in children may be caused by mitochondrial respiratory chain deficiency.** *J Pediatr* 2000;136:209–214
3. Barkovich AJ, Good WV, Koch TK, Berg BO. **Mitochondrial disorders: analysis of their clinical and imaging characteristics.** *AJNR Am J Neuroradiol* 1993;14:1119–1137
4. Oppenheim C, Galanaud D, Samson Y, et al. **Can diffusion weighted magnetic resonance imaging help differentiate stroke from stroke-like events in MELAS?** *J Neurol Neurosurg Psychiatry* 2000;69:248–250
5. Abe K, Inui T, Hirono N, Mezaki T, Kobayashi Y, Kameyama M. **Fluctuating MR images with mitochondrial encephalopathy, lactic acidosis, stroke-like syndrome (MELAS).** *Neuradiology* 1990;32:77
6. Castillo M, Kwock L, Green C. **MELAS syndrome: imaging and proton MR spectroscopic findings.** *AJNR Am J Neuroradiol* 1995;16:233–239
7. Sandhu FS, Dillon WP. **MR demonstration of leukoencephalopathy associated with mitochondrial encephalomyopathy: case report.** *AJNR Am J Neuroradiol* 1991;12:375–379

8. Basser PJ, Pierpaoli C. **Microstructural and physiological features of tissues elucidated by quantitative-diffusion-tensor MRI.** *J Magn Reson B* 1996;111:209–219

9. Webb PG, Sailasuta N, Kohler SJ, Raidy T, Moats RA, Hurd RE. **Automated single-voxel proton MRS: technical development and multisite verification.** *Magn Reson Med* 1994;31:365–373

10. Johnston MV, Hoon AH. **Possible mechanisms in infants for selective basal ganglia damage from asphyxia, kernicterus, or mitochondrial encephalopathies.** *J Child Neurol* 2000;15:588–591

11. Ohama E, Ohara S, Ikuta F, Tanaka K, Nishizawa M, Miyatake T. **Mitochondrial angiopathy in cerebral blood vessels of mitochondrial encephalomyopathy.** *Acta Neuropathol (Berl)* 1987;74:226–233

12. Yoneda M, Maeda M, Kimura H, Fujii A, Katayama K, Kuriyama M. Vasogenic edema. **Vasogenic edema on MELAS: a serial study with diffusion-weighted MR imaging.** *Neurology* 1999;53:2182–2184

13. Clark JM, Marks MP, Adalsteinsson E, et al. **MELAS: clinical and pathologic correlations with MRI, xenon/CT, and MR spectroscopy.** *Neurology* 1996;46:223–227

14. Ohshita T, Oka M, Imon Y, et al. **Serial diffusion-weighted imaging in MELAS.** *Neuroradiology* 2000;42:651–656

15. Pierpaoli C, Jezzard P, Basser PJ, Barnett A, Di Chiro G. **Diffusion tensor MR imaging of the human brain.** *Radiology* 1996;20:637–648

16. Schaefer PW, Grant PE, Gonzalez RG. **Diffusion-weighted MR imaging of the brain.** *Radiology* 2000;217:331–345

17. Huppi PS, Murphy B, Maier SE, et al. **Microstructural brain development after perinatal cerebral white matter injury assessed by diffusion tensor magnetic resonance imaging.** *Pediatrics* 2001;107:455–460

18. Ohara S, Ohama E, Takahashi H, et al. **Alterations of oligodendrocytes and demyelination of the spinal cord of patients with mitochondrial myopathy.** *J Neurol Sci* 1988;86:19–29